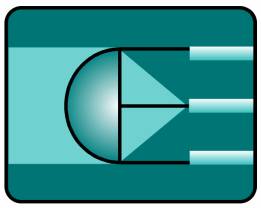

Chair of Optoelectronics

Institute for Computer Engineering

Ruprecht-Karls-University Heidelberg

Annual Report 2011

UNIVERSITÄT HEIDELBERG

Zukunft. Seit 1386.

Contents

STAFF

Prof. Dr. Karl-Heinz Brenner
Lehrstuhlinhaber

Fernando Merchán Alba
Wissenschaftlicher Mitarbeiter

Dr. Xiyuan Liu
Wissenschaftliche Mitarbeiterin

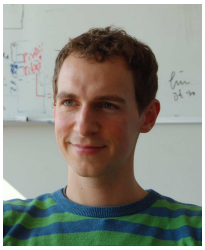

Maximilian Auer
Wissenschaftlicher Mitarbeiter

Wolfgang Stumpfs
Technischer Angestellter

Eike Slogsnat
Wissenschaftlicher Mitarbeiter

Tim Stenau
Student

Sabine Volk
Büroleitung / Sekretariat

Eva Treiber
Studentin

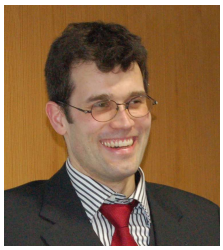

Matthias Fertig
Externer Doktorand
(IBM Forschung & Entwicklung GmbH)

Foreword

Dear reader,

This annual report describes the research activities of the chair of optoelectronics for the year 2011. Because of the participation in the Viroquant project, a large fraction of the research work directly or indirectly has to do with microscopy (7,8,11). Another growing focus of work is computational optics (1-4,10), serving as an inevitable tool for the realistic design of optical systems. In the scalar optical description, the inclusion of a tilted optical axis found an application in the treatment of micro-optical connectors. In the vectorial description, we looked at absorption as a local quantity, with the optimization of photo-detectors in mind. The extension of the initially scalar WPM to a vectorial counterpart showed good agreement with rigorous methods but with the possibility of simulating much larger structures. In one contribution, we also looked at a more academic problem - the focusing of light in a Maxwell-fisheye lens, where we found no resolution enhancement thus Abbe's law is also valid in this micro-optical regime.

We hope that this report will find your interest

Karl-Heinz Brenner
Head of the chair

Research Projects

Numerical light propagation between tilted planes

K.-H. Brenner

The numerical treatment of light propagation usually occurs between two planes perpendicular to the optical axis. Examples include the Fresnel propagation, the angular spectrum of plane waves (AS) or the Sommerfeld diffraction formula. Consequently the source plane and the destination plane are parallel. There are many situations, where one requires a propagation between non-parallel or tilted planes. For example, in tolerance analysis, one needs to now how much tilt of a lens or a detector plane is allowable for a given system configuration. Another very old example is the Scheimpflug condition, applied to reduce distortion in recording situations, where the camera looks at a tilted source plane. But also in micro optics there are several examples, where numerical light propagation between tilted planes is needed. One natural candidate is the parallel integration of optical components on a substrate surface (PIFSO) where the light propagation occurs at a 45° angle to the plane parallel surfaces. In one of our projects, the micro-integration of an optical fiber connector, we also required a numerical light propagation between tilted planes. In this project, light from a semiconductor laser falls on a 45°-mirror and is reflected towards the fiber. In order to analyse the sensitivity of this arrangement to mirror imperfections, the mirror plane had to be tilted.

The problem of light propagation has been reported by several authors, most recently in [1]. In all of these publications, the coordinate transformation from the source plane to the destination plane is treated as a single rotation around an axis - typically an elementary axis like the x- or y-axis. For a general tilt, the transformation has to be synthesized by a series of rotations around orthogonal axes, which complicates the treatment significantly.

In order to simplify this problem, we have taken a different approach. We assume, that there is a global coordinate system with the orthogonal unit vectors $\mathbf{e}_x$, $\mathbf{e}_y$ and $\mathbf{e}_z$ and we define the source and the destination coordinate system in terms of this global system. Assume, the source coordinate system is defined by the three orthogonal unit vectors $\mathbf{x}$, $\mathbf{y}$ and $\mathbf{z}$ and an origin vector $\mathbf{o}$ and likewise the destination coordinate system is defined by the three orthogonal unit vectors $\mathbf{X}$, $\mathbf{Y}$ and $\mathbf{Z}$ and an origin vector $\mathbf{O}$. Then, the mapping of a point from the source coordinate system to the destination coordinate system can be described as

$$\begin{pmatrix} X \\ Y \\ Z \end{pmatrix} = \begin{pmatrix} \mathbf{xX} & \mathbf{yX} & \mathbf{zX} \\ \mathbf{xY} & \mathbf{yY} & \mathbf{zY} \\ \mathbf{xZ} & \mathbf{yZ} & \mathbf{zZ} \end{pmatrix} \begin{pmatrix} x \\ y \\ z \end{pmatrix} + \begin{pmatrix} (\mathbf{o}-\mathbf{O})\mathbf{X} \\ (\mathbf{o}-\mathbf{O})\mathbf{Y} \\ (\mathbf{o}-\mathbf{O})\mathbf{Z} \end{pmatrix} \qquad (1)$$

The inverse operation can be determined in a similar way. The important difference to previous approaches is that no rotation matrix has to be constructed. All the quantities required for the transformation are available in the description of the unit vectors and the origins. Applying this transformation to the angular spectrum of plane waves method, we obtain

$$u(\mathbf{R}) = \frac{1}{(2\pi)^2} \iint \tilde{u}_0\left((\mathbf{t}\cdot\mathbf{K})_\perp\right) e^{i\mathbf{K}\cdot\mathbf{T}\cdot\Delta\mathbf{O}_r} e^{i\mathbf{K}\cdot\mathbf{R}} \left|\mathbf{J}_{k,K}\right| d^2K_\perp \quad (2)$$

with $\mathbf{T} = \mathbf{t}^{-1}$ as the transformation matrix and $\Delta\mathbf{O}$ as the origin difference from eq. 1. All the contributions like the propagation phase shift and the Jacobian of the transformation follow naturally from the coordinate replacement. The most imported aspect of eq. 2 is that tilted light propagation can also be treated by a standard Fourier transform, which enables a calculation which is almost as fast as the classical calculation.

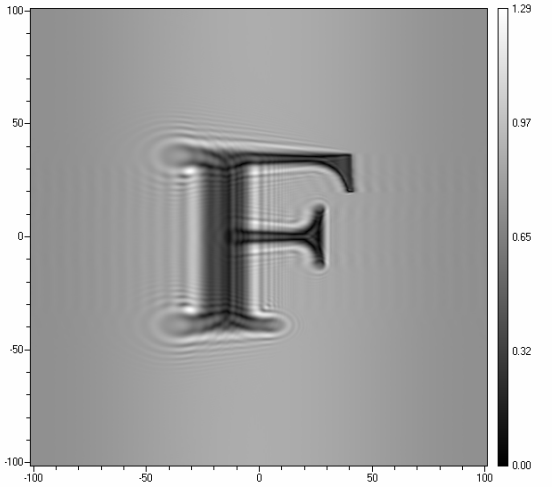

Fig. 1: Numerical light propagation of a black letter F on white background to a plane separated by 30 µm and tilted by 45°

Publications:

[1] K. Matsushima, H. Schimmel, F. Wyrowski - J. Opt. Soc. Am A, Vol. 20, No. 9, 1755 (2003)

[2] K.-H. Brenner, „Aspekte der Lichtausbreitung zwischen verkippten Ebenen", Jahrestagung der Deutschen Gesellschaft für angewandte Optik e. V. in Wetzlar (2010)

The Vector Wave Propagation Method (VWPM)
An extension to the wave propagation method

M. Fertig, K.-H. Brenner

In this project, we have extended the scalar wave propagation method (WPM) to vector fields. The WPM [1] has been introduced in 1993 in order to overcome the mayor limitations of the beam propagation method (BPM). With the WPM, the range of application could be extended from the simulation of waveguides to simulation of conventional optical elements like lenses and gratings. The WPM already provided valid results for propagation angles up to 85 degrees. For such large numerical apertures, polarization effects may become relevant Therefore, we extended the WPM to 3D-vectorial fields[2] by considering the polarization dependent Fresnel coefficients at the interfaces in each propagation step.

Theory

Similar to the WPM, the first step in the algorithm is the decomposition of the field into plane wave components. Unlike the WPM, now we treat the electric field as a three component vector. The plane wave decomposition thus is

$$\tilde{\mathbf{E}}_{\perp,m}\left(\mathbf{k}_\perp\right) = \iint \mathbf{E}_{\perp,m}\left(\mathbf{r}_\perp\right)\cdot\exp\left(-i\,\mathbf{k}_\perp\mathbf{r}_\perp\right) d^2\mathbf{r}_\perp$$

The third or the z-component is not needed, because of the transversality condition

$$E_z = -\frac{\left(E_x k_x + E_y k_y\right)}{k_z}$$

At each interface, the electric field transforms according to

$$\tilde{\mathbf{E}}_{\perp,m+1}\left(\mathbf{k}_\perp\right) = \mathbf{M}_{m,m+1}\left(\mathbf{r}_\perp,\mathbf{k}_\perp\right)\cdot\tilde{\mathbf{E}}_{\perp,m}\left(\mathbf{k}_\perp\right)$$

The transfer matrix M considers the Fresnel coefficients for transmission and is given by

$$\mathbf{M}_{m,m+1} = \frac{1}{k_\perp^2}\begin{pmatrix} k_y^2 t_s + k_x^2 \hat{t}_p & k_x k_y\left(\hat{t}_p - t_s\right) \\ k_x k_y\left(\hat{t}_p - t_s\right) & k_x^2 t_s + k_y^2 \hat{t}_p \end{pmatrix}$$

where t_s is the well known transmission coefficient for TE-polarisation and $\hat{t}_p = \frac{n_m k_{z,m+1}}{n_{m+1} k_{z,m}} t_p$ is a modified transmission coefficient for TM-polarisation. The propagation phase for one plane wave component is the same as in the WPM. The final field at the interface to the next layer is obtained by a summation over all plane wave components.

Verification

We verified the validity of this approach using several standard problems with know solutions. In the simplest case we looked at the transmission of a plane wave through a prism, where the angle change and the transmission coefficient agreed well with the exact theory. In another case, we compared the focal distribution of an unaberrated wavefront from vectorial Debye theory to the VWPM-result. Also here we obtained a good agreement.

Finally we compared the simulation of a two-dimensional dielectric grating with the results from the three-dimensional RCWA.

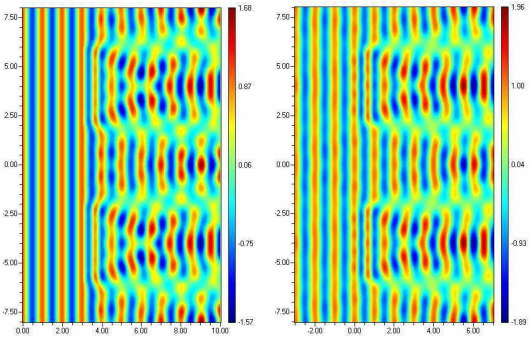

Fig. 1: Comparison of the electric fields for the VWPM (left) and RCWA (right) for a dielectric grating. The main difference is the missing reflection in the VWPM.

While the RCWA was able to calculate 10x10 modes in a reasonable time, the VWPM-result used 512x512 modes in roughly the same time.

Publications:

[1] K.-H. Brenner and W. Singer, "Light propagation through microlens: a new simulation method", Appl. Opt. **32**, 4984 - 4988, (1993).

[2] M. Fertig, K.-H. Brenner, "Vector wave propagation method (VWPM) - An extension to the wave propagation method", J. Opt. Soc. Am. A, Vol. **27**, No. 4, 709 – 717, (2010)

Rigorous simulation of the imaging properties of Maxwell's Fisheye lens

K.-H. Brenner

Recently, there has been considerable interest in the possibility of perfect imaging of Maxwell's fisheye lens. Perfect imaging has been reported before by Zhang, Pendry and others [1] for the case of double negative index materials, where the negative index material performs as an amplifier for the evanescent waves. The new interest has been stimulated though a publication [2] by Ulf Leonhardt from St. Andrews university, where he claimed, that a Maxwell's fisheye, well known from ray optics as a perfect imaging instrument, also performs perfect in the wave optical treatment. Perfect imaging in this context means that an arbitrarily small (sub-wavelength) light source will be imaged to the same size, thus breaking the Abbe resolution limit. This would be especially surprising since Maxwell's fish eye is composed of conventional gradient index material without any negative index effects.

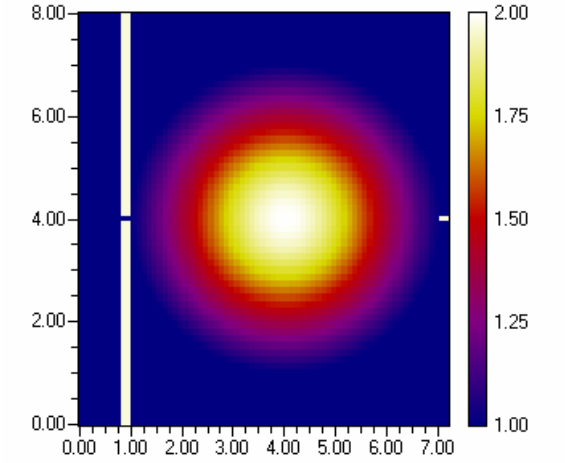

Fig. 1: Index distribution of the model geometry of the fisheye lens used in the simulation

The possibility of perfect focusing has been debated by a number of authors [3]. At the same time it appears to have been confirmed by microwave experiments. Although it may not seem very practical to use tiny spheres for high resolution imaging, the understanding of the mechanisms could lead to new and unconventional imaging systems. Therefore we looked into this subject in a very straight forward way. Because we have all the simulation tools for analysing this question readily available, we performed a simulation based on the rigorous coupled wave analysis.

The model geometry is shown in fig. 1. To generate a subwavelength sized source, we added a metal aperture of 100 nm, using 1000 nm wavelength for the source. The result of the simulation is shown in fig. 2. At first, we notice, that it is very difficult to generate a source with a diameter of $\lambda/10$. Although we used TM-polarization, the transmitted amplitude has decreased considerably compared to the incident field. The other thing to note is that the fisheye lens indeed generates an image spot, but the resolution is not below the Abbe resolution limit since the smallest features in the intensity according to Abbe should be $\lambda/2$, which agrees with the observation.

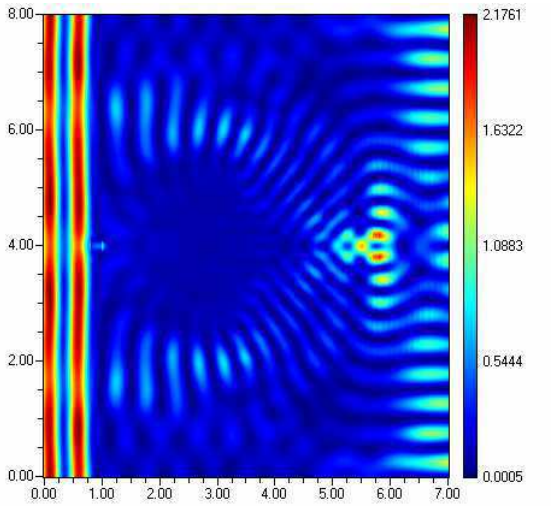

Fig. 2: RCWA simulation of light propagation in a Maxwell fisheye lens using a 100 nm aperture and a 100 nm drain

In the discussion mentioned before, Leonhardt argued that a drain in the image plane is essential for the performance. Therefore we added a metallic drain of 100 nm diameter (fig.1, right side). The result of this simulation (fig,2) showed no notable difference to the case without a drain.

Publications:

[1] K:-H: Brenner, „Plane Wave Decomposition in Layered Materials and Meta-materials“, 6th International Workshop on Information Optics, ed. J.A. Benediktsson, B. Javidi, K.S. Gudmundsson, American Institute of Physics (AIP), ISBN 978-0-7354-0463-2/07, pp 59 – 66, (2007)

[2] U. Leonhardt "Perfect imaging without negative refraction", New Journal of Physics 11 (2009) 093040.

[3] R. J. Blaikie, "Perfect imaging without refraction? New Journal of Physics 13 (2011) 125006, 1367-2630.

Implementation of an efficient finite difference method for the E-Field to calculate light propagation in the time domain

Eva Treiber, K.-H. Brenner

In the thesis of my academic studies, I am dealing with a fast and rigorous method for the numerical simulation of the propagation of light. The aim is to calculate light propagation in different systems with only real electric fields in the time domain, so there is no need for any complex treatment or the introduction of magnetic fields. This reduction is possible without loss of accuracy for monochromatic light fields.

Starting with Maxwell's equations, for isotropic and linear media we expressed the magnetic field in terms of the electric field, resulting in a differential equation only for the real part of the electric field. A discretisation of this differential equation yielded a method to directly calculate the electric field in every inner point of the discretisation region with the knowledge of the field at two previous time steps.

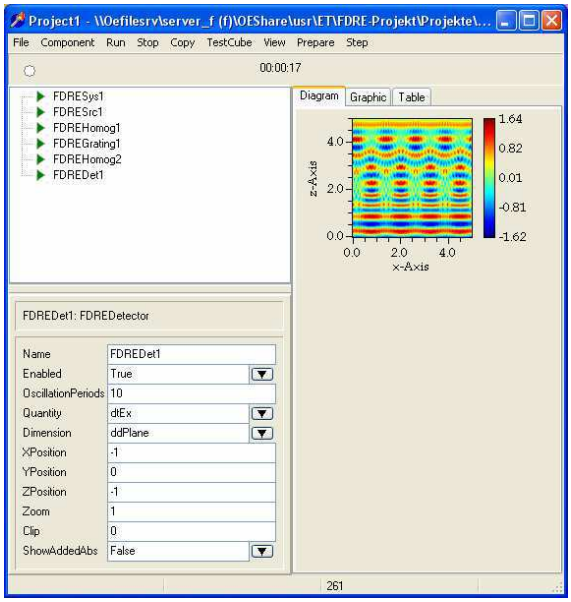

Fig. 1: User interface of the finite difference time domain simulation tool.

What was (and is) more challenging than getting the finite difference equation is the implementation of the source and the boundaries as they should represent physical reality; for example a source may be transparent or absorbing. Boundaries should indeed act as ideal absorbers and not reflect any unphysical wave back into the simulation region. The aim of the work was to enable a user to construct any system he wants from a set of elementary layers like gratings or homogeneous regions, then set the parameters of the system, the source, choose the parameters for observation and, if he wishes to, the user can watch the light propagating through the system. Fig. 1 shows the user interface. The elementary components are assembled as a tree structure in the top left corner of the window. Each component can be edited in the bottom left corner. The result of the simulation is displayed as electric field in the diagram tab of the window. The graphic- and the table-tab provide quantitative data such as transmission and reflection curves

For verification of the software, we used a simple interface between two different media, because the result is also known analytically. The result agreed very well with the theoretical results.

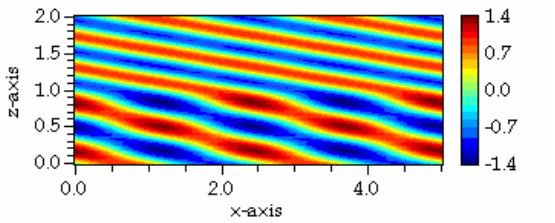

Fig 2: Verification of the software using a known problem, the reflection and transmission at a single interface

Publications:

[1] A. Unger, K.-H. Brenner, "Vergleich exakter optischer Lösungsmethoden im Zeitbereich in Hinblick auf Genauigkeit und Effizienz", DGaO-Proceedings 2008, http://www.dgao-proceedings.de, ISSN 1614-8436, 109. Jahrestagung in Esslingen am Neckar/Deutschland (2008)

Talbot length of rectangular and hexagonal gratings

X. Liu, K.-H. Brenner

The Talbot effect is a well-known optical phenomenon: self-imaging effect. When a plane wave is transmitted through a periodic structure, the propagating wave replicates its amplitude distribution at multiples of a defined distance away from the periodic structure. This distance is named the Talbot length. It is well-defined for one-dimensional (1d) periodic structures:

$$z_{Talbot} = 2P^2/\lambda \qquad (1)$$

where P is the period and λ the wavelength. For the two-dimensional case the derivation is not as straightforward as in the 1d case. In the context of a parallel scanning microscope, we have investigated the Talbot length of rectangular and also hexagonal gratings.

Since the Talbot effect is a near field diffraction effect in the paraxial approximation, it is a natural consequence of Fresnel diffraction. To determine the Talbot length, we compare the grating amplitude $|u_0|$ and its propagated amplitude $|u_z|$. It is clear, that a necessary condition of $|u_z| = |u_0|$ leads to:

$$e^{-i\pi\lambda z\left(\frac{k^2}{P_x^2}+\frac{l^2}{P_y^2}\right)} = 1 \quad \Rightarrow \quad e^{-i2\pi z\left(\frac{k^2}{2P_x^2/\lambda}+\frac{l^2}{2P_y^2/\lambda}\right)} = 1 \qquad (2)$$

Since k,l are integers, the condition above is fulfilled if and only if the smallest common multiple (LCM) of two real numbers exists:

$$z_{Talbot} = LCM\left(\frac{2P_x^2}{\lambda}, \frac{2P_y^2}{\lambda}\right) \qquad (3)$$

The LCM of two integers or rational numbers is well-defined. Here, LCM is extended to any two real numbers and if existing, LCM is the smallest real number that is an integer multiple of both of two real numbers. However, the LCM of any two real numbers may not exist. For example, one can not find a real number, which is an integer multiple of $\sqrt{3}$ and at the same time also an integer multiple of $\sqrt{5}$, therefore LCM of $\sqrt{3}$ and $\sqrt{5}$ does not exist. Hence, for an arbitrary rectangular grating, Talbot effect may or may not occur. For a square shaped 2d-grating $\left(P_x = P_y = P\right)$, the Talbot length is well-defined according to eq. 1

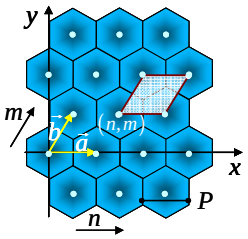

Fig. 1: A hexagonal grating and its elementary cell

For a hexagonal grating with a period P, shown in Figure 1, the necessary condition to satisfy $|u_z| = |u_0|$ is now

$$e^{-i\pi\lambda z\left(\frac{k^2}{P^2}+\left(\frac{2}{\sqrt{3}}\frac{l}{P}-\frac{1}{\sqrt{3}}\frac{k}{P}\right)^2\right)} = e^{-i2\pi\frac{z}{3P^2/2\lambda}\left(k^2+l^2-lk\right)} = 1 \qquad (4)$$

Since k,l are integers, this condition can be fulfilled if

$$z_{Talbot} = 3P^2/2\lambda \qquad (5)$$

Thus, for a hexagonal grating, self imaging always exists and the Talbot length in a hexagonal geometry is well-defined by multiples of $3P^2/2\lambda$ [1,2].

Publications:

[1] John T. Winthrop and C. R. Worthington, „Theory of Fresnel Images. I. Plane Periodic Objects in Monochromatic Light“, JOSA, vol. 55, pp 373 – 380, (1965)

[2] Peng Xi, Changhe Zhou, Enwen Dai and Liren Liu, "Generation of near-field hexagonal array illumination with a phase grating", Opt. Lett. Vol. 27, pp 228-230 (2002)

Determination of the Jones-matrix of a SLM by a Mach–Zehnder interferometer with an off-axis reference wave

X. Liu, K.-H. Brenner

The spatial light modulator (SLM) to be characterized was HOLOEYE's LC 2002, based on a translucent liquid crystal micro display with 832× 624 pixel and a pixel pitch of 32µm. The device modulates light spatially in amplitude and phase by addressing each pixel with an 8 bit grey value.

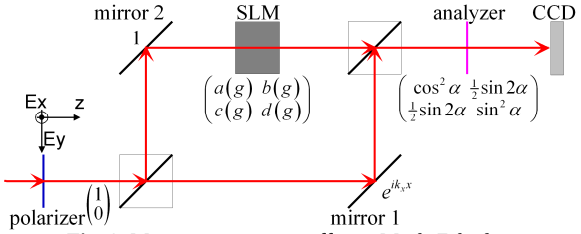

Fig. 1: Measurement setup: off-axis Mach-Zehnder interferometer

A Mach-Zehnder interferometer with an off-axis reference wave $e^{ik_x x}$ (Fig. 1) is proposed to characterize the complex modulation of the SLM by a Jones matrix, which is dependent on the given grey value g

$$\mathbf{J}(g)=\begin{pmatrix} a(g) & b(g) \\ c(g) & d(g) \end{pmatrix}, \qquad a,b,c,d \in \mathbb{C} \qquad (1)$$

The off-axis reference wave is set in such a manner that without any test object in the object path, the interference pattern on CCD shows vertical fringes (Fig. 2).

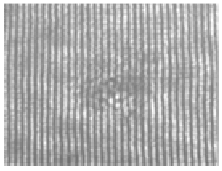

Fig. 2: Interferogram without SLM

If the SLM in the object path, is set by a grey value distribution as shown in Fig. 3 left, the contrast of interference fringes on the CCD will change and the fringe position will be shifted as shown in Fig. 3, right.

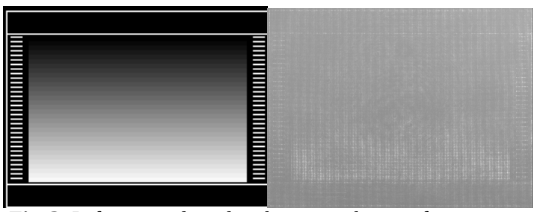

Fig. 3: Left: grey values distribution, right: interferogram on CCD

The complex Jones matrix for each grey value can then be derived from the contrast and the interference stripe shift by comparing them with the initial situation of figure 2. For each grey value, the determination of all the 4 unknown complex parameters a, b, c, d requires at least 4 independent measurements of the contrast and the fringe shift. The independent measurements are realized here by adjusting the proper polarization states of the analyzer (Fig. 1). The polarizer is set in x-direction all the time.

To determine the complex parameters a,c, the polarization state of the analyzer is set to x-direction firstly and then to $\alpha = 45°$ with respect to the x-axis. The relationship of the measured contrast values and fringe shifts to a and c can then be represented by

$$\begin{aligned} contrast_{\alpha=0} &= |a|, & shift_{\alpha=0} &= -\arg(a), \\ contrast_{\alpha=45°} &= \frac{1}{2}|a+c|, & shift_{\alpha=45°} &= -\arg(a+c). \end{aligned} \qquad (2)$$

To determine the complex parameters b,d, the SLM is rotated by 90° around the optical axis to swap the x- and y-axis of the SLM. Now in the coordinate system of the interferometer, the Jones matrix of SLM is transformed to

$$\mathbf{J}_{90°}(g)=\begin{pmatrix} d(g) & -c(g) \\ -b(g) & a(g) \end{pmatrix}, \qquad a,b,c,d \in \mathbb{C}\,. \qquad (3)$$

After the rotation of the SLM, the polarization state of analyzer is set to x-direction and then to $\alpha = 45°$ with respect to the x-axis too. The relationship between the measured parameters and the parameters to be determined are now expressed by

$$\begin{aligned} contrast_{\alpha=0} &= |d|, & shift_{\alpha=0} &= -\arg(d), \\ contrast_{\alpha=45°} &= \frac{1}{2}|d-b|, & shift_{\alpha=45°} &= -\arg(d-b). \end{aligned} \qquad (4)$$

The evaluated 4 complex parameters a,b,c,d are shown in the following graphics in dependence of the grey value.

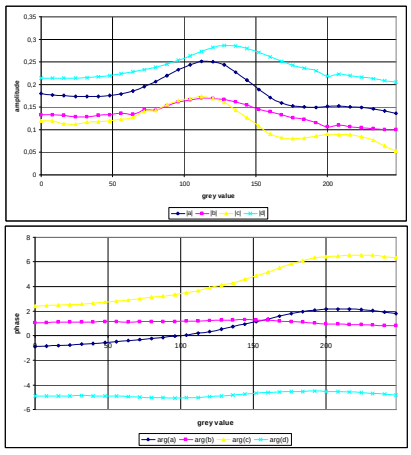

Fig. 4: Amplitude (top) and phase (bottom) of a,b,c,d .

Analysis of the Image Aberrations produced by slightly spherical dichroic Beam Splitters in the Imaging Path

E. Slogsnat, P. Fischer, K.-H. Brenner

In a concept of a parallel multi-spectral fluorescence microscope, the excitation light and the emission light have to pass several dichroic beam splitters (Fig.1).

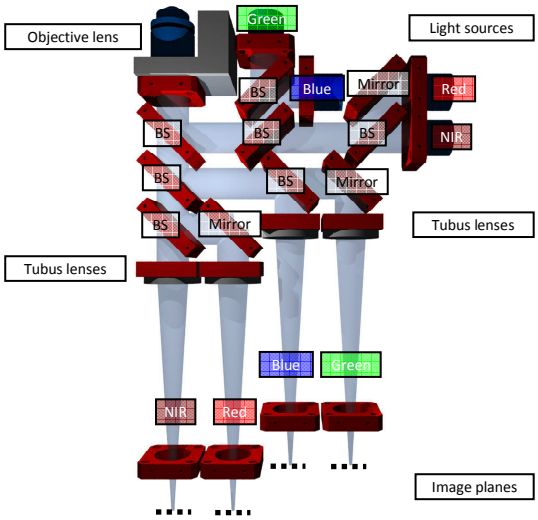

Fig. 1: Schematic setup of a parallel multi-spectral fluorescence microscope

The system is infinity corrected and all beam splitters are located in the pupil plane. Thus the light beams passing through the beam splitters are almost collimated. The objective lens has a magnification of 10 and a NA of 0.45. The focal length of all tubus lenses is 164.5 mm and the diameter of the light beams is 20 mm.

Due to the fabrication process, all beam splitters in this project have a slight, primarily spherical surface (Fig. 2).

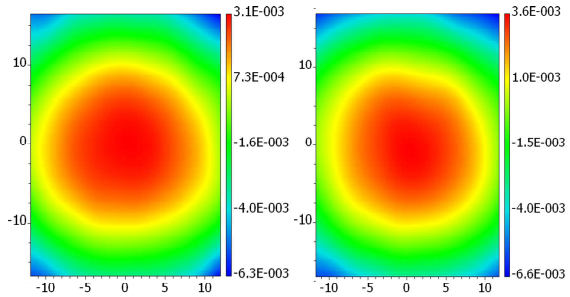

Fig. 2: Measured surface profile of two different dichroic beam splitters (units: mm)

The spherical shape would be tolerable, if the incident angle of the light was orthogonal to the beam splitter surface. In this case the spherical part of the deformation could be compensated by refocusing (Fig. 3). In this set-up, however, the beam splitters are at an angle of 45 degree with respect to the optical axis.

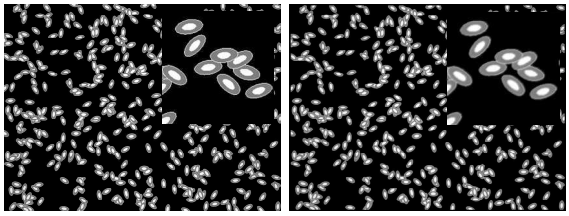

Fig. 3: Simulated images (**left:** perfect mirror; **right:** with measured surface data of beam splitter as mirror and refocusing)

In the excitation path the deformations do not play a significant role. In the imaging path there are two different scenarios: When used in transmission, they mainly produce a phase shift, which does not affect image quality. When used in reflection, the deformations produce a position-dependent defocus. Due to this local dependency the image is blurred (Fig. 4).

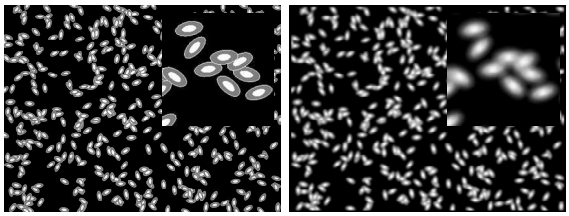

Fig. 4: Simulated images (**left:** perfect mirror; **right:** with measured surface data of beam splitter as mirror)

If an aperture is inserted behind the tubus lens, a sharper image is achieved again (Fig. 5), but this improvement is accompanied by a loss of intensity.

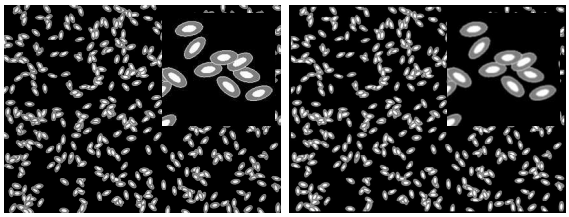

Fig. 5: Simulated images (**left:** perfect mirror; **right:** with measured surface data of beam splitter as mirror and aperture behind tubus lens)

Design of the Illumination Path in a miniaturized parallel Fluorescence-Microscope

E. Slogsnat, K.-H. Brenner

To accelerate image acquisition in systems biology, a concept of a miniaturized parallel fluorescence-microscope was designed (Fig.1). The imaging path was characterized by simulations and an experimental setup [1].

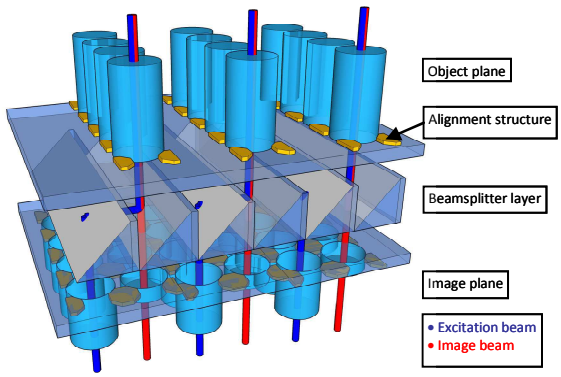

Fig. 1: Integration scheme of the miniaturized parallel fluorescence-microscope

Here a simulation of the illumination path is presented, which is designed for the fluorophore eGFP (Excitation maximum: 488 nm; Emission maximum: 507 nm). The field of view, which has to be illuminated, has a diameter of 400 µm.

Fig. 2 shows the illumination path from the light source to the object plane.

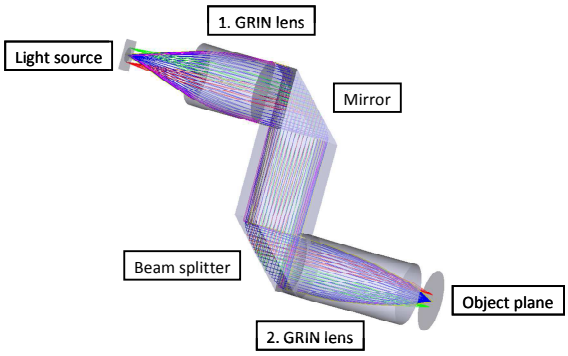

Fig. 2: Ray-trace of the illumination path of the micro-system

Since the second GRIN lens is also used in the imaging path, the only part which can be optimized is the first GRIN lens.

As light source a square Lambertian radiator with a length of the edge of 0.5 mm, a wavelength of 488 nm and a power of 1 mW is used.

The optimization goals are homogeneous illumination and low energy loss. An additional constraint was, that the light had to be almost collimated in the beam splitter layer. The optimization parameters are the length of the first GRIN lens, two fabrication parameter of the lens and the distance of the light source.

Fig. 3 shows the simulated intensity distribution in the object plane. Considering the reflexion and transmission loss, the energy efficiency is about 33 %.

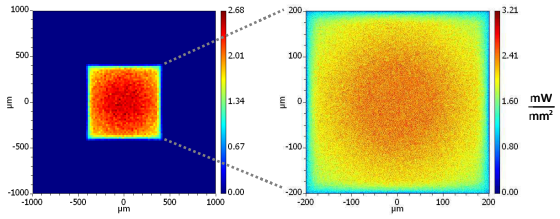

Fig. 3: Intensity distribution inside the field of view

Due to the light source's characteristics, a homogenous illumination of the Field of View can only be reached by using additional optical components. The main part of the energy loss is produced by the beam splitter, which is essential for combining the illumination and imaging paths. Nevertheless an energy efficiency of about 33 % could be reached, which was enough to realize an illumination system using LEDs with high optical output power. Using GRIN-rods with a diameter of 2 mm, the total system size is smaller than a cube of 1 cm length.

Publications:

[1] E. Slogsnat, R. Buschlinger, K.-H. Brenner, „Miniaturisierte parallele Mikroskopie in der Systembiologie", DGaO-Proceedings (Online-Zeitschrift der Deutschen Gesellschaft für angewandte Optik e. V.), ISSN: 1614-8436, 111. Jahrestagung in Wetzlar (2010)

[2] E. Slogsnat, K.-H. Brenner, „Design des Beleuchtungspfads für ein miniaturisiertes paralleles Fluoreszenz-Mikroskop", (Online-Zeitschrift der Deutschen Gesellschaft für angewandte Optik e. V.), ISSN: 1614-8436-urn:nbn:de:0287-2011-P00x-x, 112. Jahrestagung in Ilmenau (2011)

Monolithic fabrication of optical micro systems

F. Merchán, K.-H. Brenner

Recent works have confirmed the replication of metal masters as a very accurate and cost effective method for the fabrication of optical micro-devices. In fig. 1 the fabricated metal master for a modern multi-channel system is shown. In this application we use the direct replication of metal masters for the fabrication of an optical coupler. The applicability of this method in micro-integrated systems makes it attractive for the development of new concepts as we present in the following.

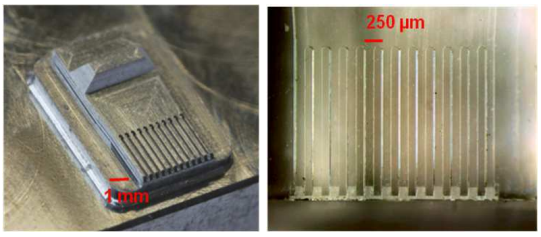

Fig. 1: Metal master for the multi-channel system(left) and optical coupler (right)

According to Moore's law, the number of transistors that can be placed in a volume unit and thus the performance doubles every two years. Modern supercomputers achieve some Peta-FLOPS (10^{15} Floating point operations per second). The requirements for data transfer between devices grow correspondingly. At bandwidths above 1 GHz, electrical transmission lines show high losses, therefore electrical signals can be transmitted only over very short distances (some cm) with an acceptable quality.

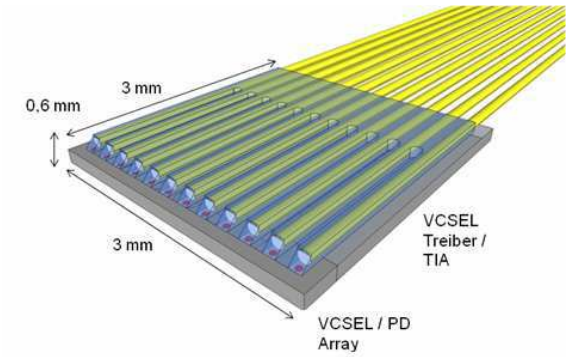

Fig. 2: Optical systems fabricated directly on the arrayed electronics

This problem can be overcome by converting the electrical signal into an optical one. Independent of the application, the development of an integrated solution is nowadays unavoidable, in order to transmit high data rates over distances up to 100 meters.

In our concept, which is based on the coupling of a laser beam to a fiber using a mirror that redirects the beam by 90° [1], it is possible to integrate high speed microelectronics and micro-optical systems in a very small volume as shown in the fig. 2.

A solution that is suitable for industrial use requires a high reproducibility and cost effectiveness of the fabrication process. A PDMS (Polydimethylsiloxan) negative master fabricated from a metal positive master is UV-transparent enabling the replication of its shape on microchips, that are connected using e.g. a BGA (Ball Grid Array) package.

VCSELs and laser drivers for the sender or photodiodes and transimpedance amplifiers for the receiver are embedded in a single chip. Modern systems reach transmission rates of 12,5 Gigabits per second. A 12 channel system would have a data rate of 300 Gbps duplex.

New developments in the area of chip packaging make an effort for integrating several functional blocks like electrical connections, memory units, a processor unit, a logic device and the optoelectronic devices in a single package. A sketch of the concept is shown in the fig. 3, in which additionally, the optical system is integrated in the package. As result, a compact computing unit working at very high speeds is no longer limited by the bandwidth of electrical transmission lines.

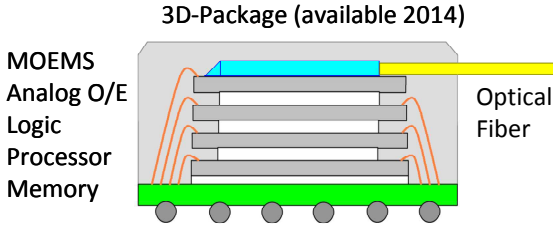

Fig. 3: Possible future developments

Publications:

[1] F. Merchán, K.-H. Brenner, "Neuartiges Integrationskonzept für kostengünstige Herstellung optischer Mikrosysteme", DGaO-Proceedings (Online-Zeitschrift der Deutschen Gesellschaft für angewandte Optik e. V.),ISSN: 1614-8436, 112. Jahrestagung in Ilmenau, (2011)

Aspects for calculating local absorption with the rigorous coupled-wave method

M. Auer and K.-H. Brenner

The Rigorous Coupled Wave Analysis (RCWA) is a method for the rigorous solution of the Maxwell's equations. It can be used to calculate the interaction between electromagnetic fields and periodic nanostructures, like optical gratings.

In most applications only the diffraction coefficients and efficiencies are the relevant quantities. Using the law of energy conservation, one can easily determine the *Global Absorption* from these quantities:

$$\text{Global Absorption} = 1 - \text{Transmission} - \text{Reflection} \quad (1)$$

The reasons for calculating the electromagnetic near fields on the other hand are mostly for visual display. In some newer applications though, like in the design and optimization of solar cells and extremely compact detectors, the *Local Absorption*, which is directly connected to the local fields, plays an important role. The relative absorbed and integrated power[1] is:

$$\frac{P_a}{P_{inc}} = \frac{k_0^2}{k_{inc,z}} \frac{1}{A} \iiint_V \mathrm{Im}\left(\varepsilon(\mathbf{r})\right) \left|\mathbf{E}_1(\mathbf{r})\right|^2 dV \quad (2)$$

The characteristics of the fields, however, strongly depend on a calculation time critical factor, which is the number of modes (or resolution of the frequency domain). In order to be able to calculate realistic fields even with a small mode count, different methods of field calculation were presented in the past. But this way the EM-fields, which are derived from the RCWA, are not unique anymore. Here the theory of *Local Absorption*[1] provides a quantitative reference criterion as the following law must apply:

$$\text{Global Absorption} - \iiint_V \text{Local Absorption}(\mathbf{r})\, dV = 0 \quad (3)$$

For a homogeneous absorbing medium, *Global Absorption* and integrated *Local Absorption* are perfectly consistent, when calculating the local fields with the standard method (cf. fig1).

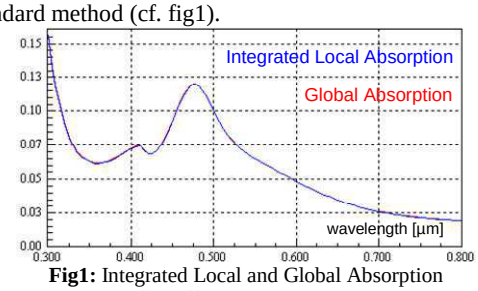

Fig1: Integrated Local and Global Absorption for different wavelengths

For a structured absorbing medium (cf. fig2) though the two quantities agree only roughly (cf. fig3a/b). While in case of TE polarization the deviation can still be explained by the discretization of the simulation area, in the TM-case there is a systematic error.

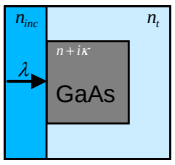

Fig2: Geometry of a unit cell

A closer look on how the 2D-RCWA calculates the fields by default[4] shows that in all equations material parameters only occur as mode-limited and thereby continuous quantities. However, for the x-component of the electric field at a boundary surface, Maxwell only demands the continuity of the tangential components. But due to the material discontinuity at the boundaries one would also expect discontinuity of the electric field in normal direction.

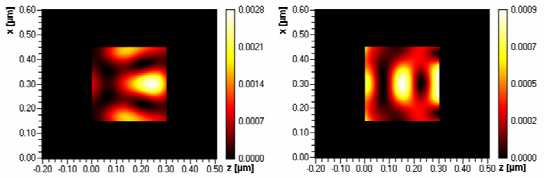

Fig3a: Local. Abs., TE-Pol.
Global Absorption: 3.540%
Integr. Loc. Abs.: 3.535%
Error: 0.14%

Fig3b: Local. Abs., TM-Pol.
Global Absorption: 1.389%
Integr. Loc. Abs.: 1.479%
Error: 6.48%

Therefore Lalanne, Jurek[5] derived the x-component from the continuous D-field and then multiplied with the local permittivity ε(**r**), in order to obtain the desired discontinuity. A method by Brenner[6] likewise derives the x-component from the continuous D-field, but then multiplies with the mode-limited permittivity.

$$E_x(x,z) = \sum_m e_m(z) \exp\left(ik_{x,m}x\right) \qquad \mathbf{e}(z) = -i \cdot \mathbf{E_a WQD}(z) \quad (4)$$

$$E_x(x,z) = \frac{1}{\varepsilon(x)} \sum_m d_m(z) \exp\left(ik_{x,m}x\right) \qquad \mathbf{d}(z) = -i \cdot \mathbf{WQD}(z) \quad (5)$$

$$E_x(x,z) = \sum_m e_m(z) \exp\left(ik_{x,m}x\right) \qquad \mathbf{e}(z) = -i \cdot \mathbf{E}^{-1}\mathbf{WQD}(z) \quad (6)$$

(4): Standard method, (5): Lalanne & Jurek, (6): Brenner

Using (3) as a target function, now the different approaches can be compared. Fig.4 shows that both improvements lead to significantly more consistent results.

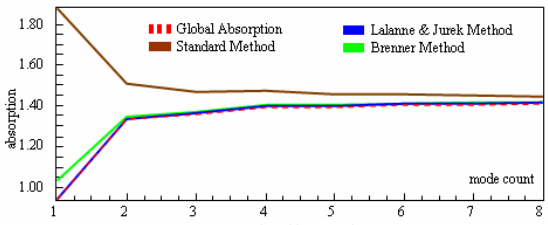

Fig4: convergence behavior of different field calculation methods

Publications:
[1] Brenner, K.-H. "Aspects for calculating local absorption with the rigorous coupled-wave method" Optics Express, Vol. 18, Issue 10, pp. 10369-10376 (2010)

Theoretical, numerical and experimental analysis of a new concept for parallel scanning microscopy

T. Stenau

A new parallel scanning microscope as a non-imaging technology, which contains micro and macro optical components, is developed in a diploma thesis and was presented at the annual general meeting of the DGaO 2011 [1]. The concept is shown in figure 1.

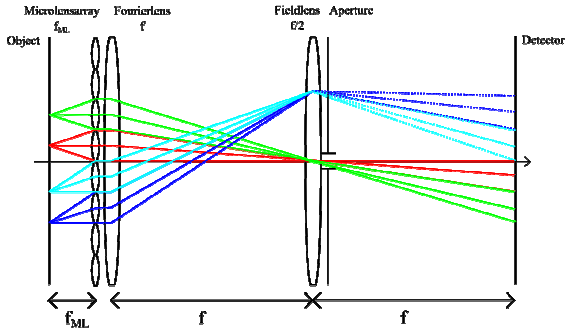

Fig. 1: Path of rays of the concept

A micro lens array combined with a movable aperture images objects in the focus of the micro lenses on a detector. The image on the detector without the aperture is a superposition of all object points in front of the micro lenses, the aperture filters which points of the focal plane of the micro lens array are detected.

The system is analysed with scalar optical simulation tools and and in an optical experiment. Different illuminations are compared and it is discussed whether the micro lens array can be replaced by a phase-step array.

The experiment showed that best results are achieved by using a spatially incoherent source such as an OLED instead of an LED or a coherent light source as the illuminating system, see figure 2.

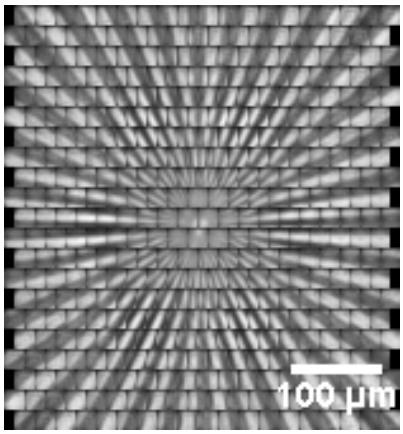

Fig. 2: Result of the experiment with an OLED as illuminating source

The experimentally achieved resolution using a micro lens array was measured as 3.4 ± 0,2 µm. This resolution is close to the Rayleigh limit of 3.0 ± 0,2 µm and confirms the theoretical values, so the capabilities of this new system are validated.

Publications:

[1] T. Stenau, X. Liu, K.-H. Brenner, „Analyse eines neuen Systemkonzepts zur parallel scannenden Mikroskopie“, DGaO-Proceedings (Online-Zeitschrift der Deutschen Gesellschaft für angewandte Optik), ISSN 1614-8436-urn:nbn:de:0287-2011-P005-9, 112. Jahrestagung, 14.-18. Juni 2011, Ilmenau, (2011)

Publications

1. M. Auer, K.-H. Brenner, „Enhancement of Photodetector Responsivity in Standard SOI CMOS Processes by introducing Resonant Grating Structures”, JEOS:RP 6, 110145 (2011)
2. F. Merchán, K.-H. Brenner, "A concept for the assembly and alignment of arrayed microelectronic and micro-optical systems for Optical Multi-Gigabit Communication", *Optoelectronic Interconnects and Component Integration XI Conference OE112*, 22.-27.01.2011, San Francisco, California, USA, Proc. of SPIE Vol. 7944, 79440D · © 2011
3. K.-H. Brenner, R. Buschlinger, „Parallel image scanning with binary phase gratings“, Journal of European Optical Society : Rapid Publications 6, 11024 (JEOS:RP), ISSN 1990-2573, (2011)
4. K.-H. Brenner, “ Aspekte der Lichtausbreitung zwischen verkippten Ebenen ”, *DGaO-Proceedings* (Online-Zeitschrift der Deutschen Gesellschaft für angewandte Optik e. V.), ISSN: 1614-8436-urn:nbn:de:0287-2011-B009-2, 112. Jahrestagung, 14.-18. Juni 2011, Ilmenau, (2011)
5. F. Merchàn, K.-H. Brenner, „Monolithisches Fertigungskonzept für die kostengünstige Herstellung optischer Mikrosysteme“, (Online-Zeitschrift der Deutschen Gesellschaft für angewandte Optik e. V.), ISSN: 1614-8436-urn:nbn:de:0287-2011-B004-0, 112. Jahrestagung, 14.-18. Juni 2011, Ilmenau, (2011)
6. T. Stenau, X. Liu, K.-H. Brenner, „Analyse eines neuen Systemkonzepts zur parallel scannenden Mikroskopie“, (Online-Zeitschrift der Deutschen Gesellschaft für angewandte Optik e. V.), ISSN: 1614-8436-urn:nbn:de:0287-2011-P005-9, 112. Jahrestagung, 14.-18. Juni 2011, Ilmenau, (2011)
7. E. Slogsnat, K.-H. Brenner, „ Design des Beleuchtungspfads für ein miniaturisiertes paralleles Fluoreszenz-Mikroskop“, (Online-Zeitschrift der Deutschen Gesellschaft für angewandte Optik e. V.), ISSN: 1614-8436-urn:nbn:de:0287-2011-P001-1, 112. Jahrestagung, 14.-18. Juni 2011, Ilmenau, (2011)
8. INVITED: K.-H. Brenner, „Parallel non-mechanical image scanning with micro lenses and binary phase gratings”, 10th Euro-American Workshop on Information Optics (WIO 2011), 20.-24. Juni 2011, Benicassim / Spanien, (2011)

Imprint

Publisher:

Prof. Dr. Karl-Heinz Brenner
Chair of Optoelectronics
Institute for Computer Engineering (ZITI)
Ruprecht-Karls-University Heidelberg
B6, 23-29, Bauteil C
68131 Mannheim
GERMANY

☎ +49 (0) 621 181 2700
🖷 +49 (0) 621 181 2695
💻 http://oe.ziti.uni-heidelberg.de

Layout: Sabine Volk

Kind of publication: Online

Publication date: 2013